Microflow of fluorescently labelled red blood cells in tumours expressing single isoforms of VEGF and their response to VEGF-R tyrosine kinase inhibition

Simon AKERMAN[1], Constantino Carlos REYES-ALDASORO[2]*, Matthew FISHER[2], Katie L. PETTYJOHN [2], Meit A BJÖRNDAHL[2], Helen EVANS[2] and Gillian M. TOZER[2]

* Corresponding author: Email: c.reyes@sheffield.ac.uk
1: Department of Neurology, University of California, San Francisco, 505 Parnassus Avenue, Box 0114, San Francisco, CA 94143, USA
2: Cancer Research UK Tumour Microcirculation Group, Department of Oncology, The University of Sheffield, K Floor, School of Medicine & Biomedical Science, Beech Hill Road Sheffield S10 2RX, UK

Abstract: In this work we studied the functional differences between the microcirculation of murine tumours that only express single isoforms of vascular endothelial growth factor-A (VEGF), VEGF120 and VEGF188, and the effect of VEGF receptor tyrosine kinase (VEGF-R TK) inhibition on their functional response to the vascular disrupting agent, combretastatin A-4 phosphate (CA-4-P). We used measurement of fluorescently-labelled red blood cell (RBC) velocities in tumour microvessels to study this functional response. RBC velocity for control VEGF120-expressing tumours was over 50% slower than for control VEGF188-expressing tumours, which may be due to the immature and haemorrhagic vasculature of the VEGF120 tumour. After chronic treatment with a VEGF-R tyrosine kinase inhibitor, SU5416, RBC velocities in VEGF120 tumours were significantly increased compared to control VEGF120 tumours, and similar to velocities in both VEGF188 treatment groups. Control and SU5416 treated VEGF188 tumours were not different from each other. Treatment of VEGF120 tumours with SU5416 reduced their vascular response to CA-4-P to a similar level to the VEGF188 tumours. Differential expression of VEGF isoforms not only affected vascular function in untreated tumours but also impacted on response to a vascular disrupting drug, CA-4-P, alone and in combination with an anti-angiogenic approach involving VEGF-R TK inhibition. Analysis of RBC velocities is a useful tool in measuring functional responses to vascular targeted treatments.

Keywords: Red Blood Cell Velocity, Microcirculation, Tumour Vasculature, Keyhole Tracking Model

1. Introduction

Vascular endothelial growth factor-A (commonly known as VEGF)(Ellis & Hicklin, 2008) is the predominant protein involved in normal and tumour angiogenesis, a process crucial for the supply of oxygen, nutrients and growth factors to tumours (Folkman, 1990). The VEGF gene undergoes alternative splicing to produce multiple functional isoforms, such as 121, 165 and 189 in human (Tischer *et al.*, 1991) and 120, 164, and 188 in the mouse (Shima *et al.*, 1996). Fibrosarcoma cell lines have been developed to express single isoforms of VEGF and used to study their roles in tumour vascularisation. Tumours expressing only VEGF120 are well vascularised, but present with immature blood vessels that are fragile and leaky and the tumours are prone to haemorrhage, particularly when grown in the dorsal skin-flap window chamber model, where vessels struggle to penetrate beyond the tumour edge (Tozer *et al.*, 2008). VEGF188 expressing tumours have a lower vascular volume than VEGF120 tumours, but the blood vessels are much more mature, showing good levels of pericyte coverage and less haemorrhage (Tozer et al., 2008).

Vascular disrupting agents (VDAs) are a group of compounds that selectively target tumour vasculature and cause a devastating collapse of blood flow in solid tumours, culminating in tumour cell death. It is thought

that VDAs preferentially target immature tumour blood vessels, with most evidence derived from VDAs that are tubulin-binding and endothelial cytoskeleton disrupting (Tozer *et al.*, 2005b). Disodium combretastatin A4 3-*O*-phosphate (CA-4-P) is the lead tubulin-binding VDA and studies have shown that VEGF120 tumours that present with immature vessels showed reduced vascular and growth response to CA-4-P, compared with VEGF188 tumours that possess a more mature vascular network (Tozer et al., 2008).

The VEGF receptor family of proteins belong to the protein tyrosine kinases that regulate multiple cellular processes that contribute to tumour development and progression, including cell proliferation, differentiation and cell survival (Baselga, 2006, Blume-Jensen & Hunter, 2001), and many human tumours exhibit aberrant tyrosine kinase activity that drives their growth. Tyrosine kinase inhibitors therefore represent attractive anti-tumour or anti-vascular targets in the clinic (Arteaga, 2003, Baselga, 2006). Several multi-target tyrosine kinase inhibitors that include targeting VEGF receptors have reached clinical practice or are in clinical trial (Faivre *et al.*, 2007, Drevs *et al.*, 2007). Under some dosing strategies, treatment with VEGFR-2 receptor antibodies or small molecule inhibitors can result in tumour vascular 'normalisation', whereby vascular morphology is altered and blood flow is improved over a limited time-frame (Winkler *et al.*, 2004, Jain, 2003, Jain, 2005). However, very little is known about how chronic tyrosine kinase inhibitors affect the function and morphology of the surviving blood vessels in tumours, and how this affects subsequent treatment stratagems. We sought to investigate the effects of tyrosine kinase receptor inhibition on the development of tumours expressing single isoforms of VEGF, and their subsequent response to CA-4-P treatment.

2. Methods

All experiments were conducted in accordance with the United Kingdom Home Office Animals (Scientific Procedures) Act 1986 and with local ethical approval. CA-4-P was kindly provided by Professor GR Pettit, Arizona State University.

2.1 VEGF isoform cell lines and tumours

Development of cell lines is described previously (Tozer et al., 2008), but briefly, primary mouse embryo fibroblasts expressing only single isoforms of VEGF (120, 164 or 188) or all isoforms were isolated from 13.5 days post-coitum (dpc) embryos produced by heterozygous breeding pairs of single VEGF isoform-expressing mice on a Swiss background. Fibroblast cultures were genotyped, as described (Vieira *et al.*, 2007), to identify wild-type samples and those homozygous for the $Vegfa^{120}$, $Vegfa^{164}$ or $Vegfa^{188}$ allele. Fibroblasts were immortalised and oncogenically transformed by retroviral transduction with SV40 and HRAS (*h*-ras) (Parada *et al.*, 1984, Greco *et al.*, 2005). In this study we used only VEGF120 and 188 tumours as they present with the widest functional and morphological diversity for comparison.

2.2 Window Chambers

All surgery was carried out on male severe combined immunodeficiency (SCID) mice (12-16 week-old, 28-32g) under general anaesthesia using intraperitoneal (i.p) injection of fentanyl citrate ($0.8 mg \bullet kg^{-1}$) and fluanisone ($10 mg \bullet kg^{-1}$; Hypnorm, Janssen Animal Health) and midazolam ($5 mg \bullet kg^{-1}$; Hypnovel, Roche, Welwyn Garden City, UK). Animals were kept warm during surgical procedure, and aseptic technique was used throughout. Surgical procedures are similar to those described previously (Tozer *et al.*, 2005a). Briefly, animals were shaved, depilated and a 15 mm diameter circular area of dorsal skin was removed, as well as the subcutaneous (s.c.) fat and connective tissue of the opposing skin layer, leaving the exposed panniculus muscle. An aluminium

window chamber (total weight ~2g), designed to hold two parallel windows, was implanted onto the dorsal skin. A tumour fragment (~0.5 mm in diameter, either VEGF120 or 188) from a donor animal was implanted onto the exposed panniculus muscle and the chamber was closed with a glass window to provide a depth of 200 μm for tumour growth. Sub-cutaneous dextrose saline and intraperitoneal buprenorphine (Vetergesic) were used to aid recovery and animals were kept in a warm room, 28-30 °C, until the day of experiment. Animals were grouped for treatment and received either the VEGF-R tyrosine kinase inhibitor, SU5416 (50 $mg \cdot kg^{-1}$, at a concentration of 25 $mg \cdot ml^{-1}$ subcutaneously) or vehicle control (50 μl of DMSO per mouse) as used previously (Fong *et al.*, 1999) starting at day 3 after implant, and then given every 4th day until further experimentation.

2.3 Red Blood Cell labelling

Donor red blood cells (RBC) were obtained via cardiac puncture from donor male SCID mice and labelled with the fluorescent dye 1,1', di-octadecyl-3,3,3'3'tetramethylindocarbocyanine perchlorate (DiI) (Molecular Probes, Cambridge Biosciences, UK) for the measurement of RBC velocity in the tumour vasculature. The labelling method has been published previously (Unthank *et al.*, 1993), but briefly the RBCs were separated from blood plasma and white blood cells by centrifugation and the isolated and washed RBCs incubated with DiI for 30 mins. 25 μg of DiI was used per 50 μl of packed RBCs. After incubation the RBCs were washed and resuspended in phosphate buffered saline (50 $\mu l \cdot ml^{-1}$ RBC-DiI complex). The labelled cells were kept for 3 days at 4 °C.

2.4 Intravital Microscopy

Intravital microscopy permits the observation of RBC movement in microvessels of small animals under both normal and pathological conditions (Sandison, 1924). The analysis of RBC velocities is used in many areas of research, to measure the responsiveness to vasoactive drugs (Prazma *et al.*, 1989) or response to vascular disrupting agents (Tozer *et al.*, 2001). Approximately 7-11 days after surgery, when the tumours reached ~3.0 mm in diameter, mice were given 0.2 ml (i.v.) of the RBC-DiI complex and treated with a single dose of the vascular disrupting agent, CA-4-P ($30mg \cdot kg^{-1}$, iv at a concentration of 3 $mg \cdot ml^{-1}$ in 0.9 % NaCl) and monitored for 24 hours to observe changes in RBC velocity. An inverted Nikon Eclipse E600FN fluorescence microscope with modified stage to take mice was used. Tumours were viewed at various time points over the 24 hrs after treatment (0, 2.5, 15, 30 and 60 mins, and 3, 6 and 24 hrs) under transmitted light for morphological vessel analysis, and then under epi-fluorescence illumination using a 100 W mercury arc lamp for measurement of RBC velocity, where videos were taken for 60s at each time point for analysis. Fluorescence was set up to excite at 550nm and detect the emissions at 565nm from the labelled RBCs using a custom-made fluorescence cube (Nikon, UK).

2.5 Velocity Analysis

RBC velocities were calculated from data recorded at x20 magnification with the same region of interest used at each time point. Velocities were calculated using a keyhole tracking algorithm performed in Matlab, as described previously (Reyes-Aldasoro *et al.*, 2008).

The tracking algorithm consisted of three main steps: *pre-processing* which transformed the videos into a sequence of binary images that contained segmented foreground objects (RBCs). Computational complexity (number of operations and time required to process) was reduced by reducing the number of pixels processed: alternate rows were discarded and for every row, contiguous pixels were averaged and their mean value assigned to a new pixel. Besides reducing the dimensions, a

smoothing effect was produced and noise was reduced. Intensity inhomogeneity was removed by equivalent background subtraction and artefacts, such as the labels on the screen were removed with a mean image of the temporal sequence. The centroids of the RBCs were determined together with the distances that separated them from neighbours, if any. *Tracking*, which linked the objects in contiguous frames to form the tracks by means of a keyhole model, which predicted the most probable landing position of a RBC at time *t+1* from the position in times *t-1* and *t*. The most probable step for a RBC that is moving from frame t-1 to frame t, is to follow the direction of the previous steps with the same velocity to frame t+1. If we assume that a child RBC will move with the same direction and velocity as its parent, we can predict its landing position. Of course, this would not cover changes in speed, turns in vessels or even simple movements within a wide vessel. Two regions of probability where the RBC is most probable to land were therefore defined: a narrow wedge (60° wide) oriented towards the predicted landing position, and a truncated circle (300°) that complements the wedge; together they resemble a keyhole. Once all segmented RBCs had been examined for possible parent-child relationships, a reduced number of them formed a series of tracks of different lengths. *Post-processing* removed links in tracks that could have resulted from noise, and joined sections that were considered to be split sections from a single track. The same keyhole model was used analysing the movement backwards. That is, the same keyhole model used child (t+1) and grandchild (t+2) to generate a keyhole at time (t). If the RBC of a previous time point was found to land inside the keyhole, it remained as part of the track, otherwise it was removed. Finally outliers were removed: those tracks whose average velocity exceed 3 times the standard deviation from the mean average velocity of the whole distribution were discarded. This process relies on the probability of RBC movement and allows analysis of all cells over a time period rather than a select few.

Velocity was calculated at $\mu m \cdot s^{-1}$ from the number of video frames taken for each red cell to travel between two points of measured distance. The average was weighted according to the length of each track to avoid biasing from small tracks. Fig. 1a shows a sample fluorescence image where the bright spots describe RBCs and colour lines describe the tracks that were detected at that frame (the tracks spanned several frames) and Fig. 1b shows all the tracks detected for a video sequence.

2.6 Statistics

Statistical analysis was performed using SPSS version 11.0.2 for the Apple Macintosh. Data are presented as mean ± standard error of the mean. Student's unpaired *t*-test was used to test for significant differences between two groups. Time-course experiments were measured using a mixed design ANOVA for repeated measures with between subjects factors used for tumour type and VEGF-R tyrosine kinase receptor inhibitor treatment, followed by Tukey (HSD) *post-hoc* tests correction.

3. Results

At the 0 min time-point, immediately prior to CA-4-P injection, the RBC velocity of VEGF120 tumours treated with vehicle was 188 ± 4 $\mu m \cdot s^{-1}$ which was significantly lower than the VEGF-R tyrosine kinase inhibitor-treated VEGF120 tumours, 389 ± 7 $\mu m \cdot s^{-1}$ and both VEGF188 tumour groups (untreated, 354 ± 7 $\mu m \cdot s^{-1}$ and treated 344 ± 6 $\mu m \cdot s^{-1}$). There was no significant difference with tests between any of the pairs from the three experiments VEGF188 control, VEGF188 + SU5416 and VEGF120 + SU5416 (Fig. 2).

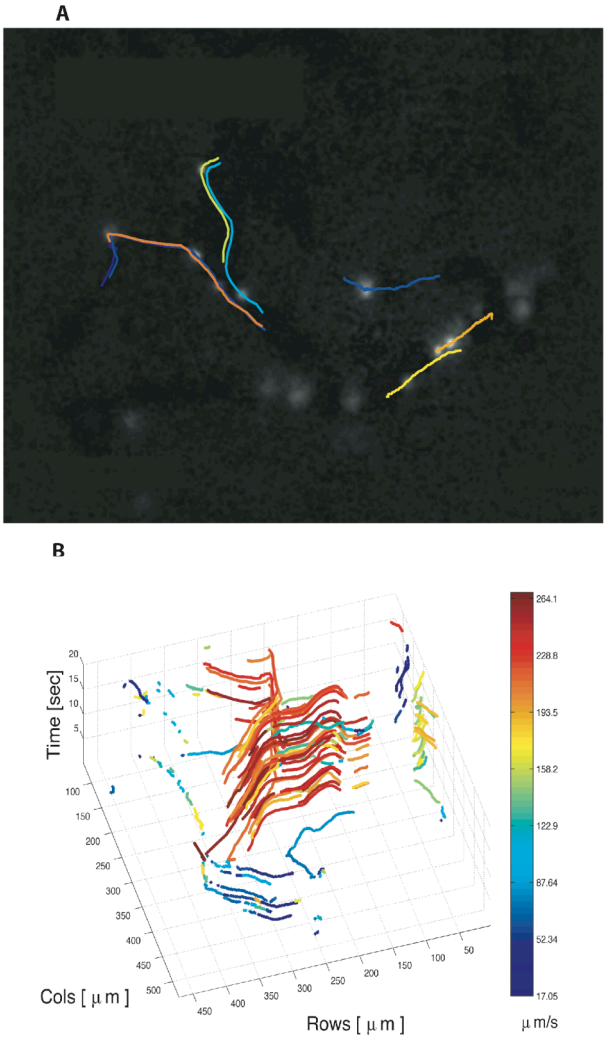

Fig 1 Tracks obtained from a video sequence. (a) A single frame with several RBCs and 6 tracks detected at this frame. (b) All the tracks detected in the video as a 3D plot with time as the z-axis. Colour of the tracks denotes the velocity

The time-course of RBC velocity response to CA-4-P, for the different tumour types ± SU5416 treatment, is shown in Figure 3. Control VEGF120 tumours without SU5416 pre-treatment, were much more responsive to CA-4-P than VEGF188 tumours, as shown previously (Tozer et al., 2008).

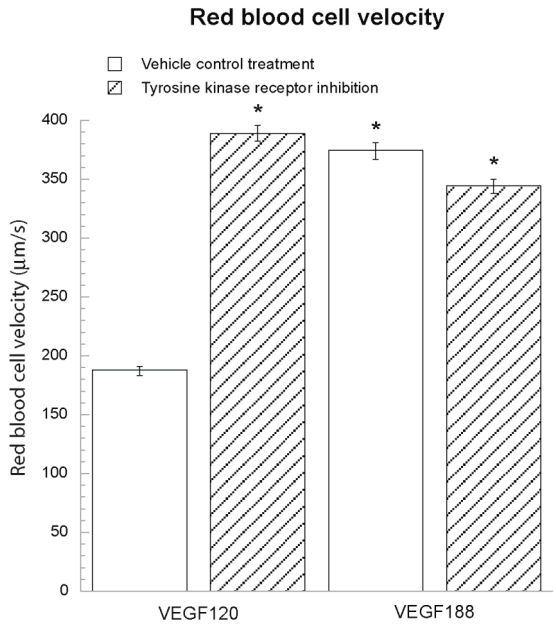

Fig. 2 Quantitative analysis of average RBC velocity of tumours grown within the dorsal skin-flap window chamber, just prior to CA-4-P treatment. Results indicate that the receptor tyrosine kinase inhibitor, SU5416, significantly increased RBC velocity in VEGF120 tumours to similar levels as VEGF188 tumours. SU5416 treatment had no effect on RBC velocity in VEGF188 tumours. * represents $P < 0.05$ significance compared to VEGF120 untreated tumours.

In VEGF120 tumours, RBC velocity was reduced to approximately 20% of its pre-treatment value by 3 hours after CA-4-P and did not recover within 24 hours, whereas, in VEGF188 tumours, RBC velocity was reduced to no more than 60% of pre-treatment level and fully recovered to pre-treatment level by 24 hours. However, SU5416 pre-treatment significantly reduced the effect of CA-4-P in the VEGF120 tumours ($P < 0.05$) (Fig. 3a), such that RBC velocity had returned to control values by 3 hours after CA-4-P treatment. In VEGF188 tumours, SU5416 pre-treatment also significantly decreased the RBC velocity response to CA-4-P ($P < 0.05$), even though this tumour type was intrinsically more resistant to CA-4-P than the VEGF120 tumours (Fig. 3b).

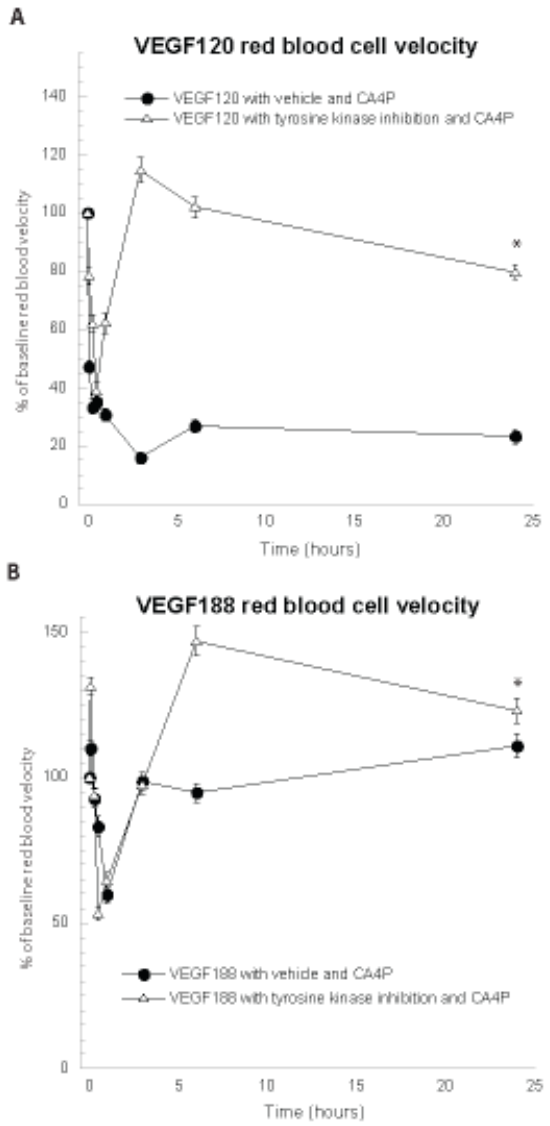

Fig. 3 Quantitative analysis RBC velocities of tumours grown in the dorsal skin-flap window chamber. Repeated measures analysis indicate significant differences between treatment groups for both VEGF120 and VEGF188 tumours for RBC velocities. * represents $P < 0.05$ for the difference between groups receiving VEGF-R TK inhibition and vehicle controls.

Between subjects comparison of VEGF120 and VEGF188 tumour responses indicates that untreated tumours were significantly differently from each other across the 24 hr time course for RBC velocities ($F_{1,16} = 8.62$, $P < 0.05$) whereas the responses of tumour lines treated with SU5416 were not significantly different from each other. It was also found that the responses of SU5416 treated VEGF120 tumours were not significant from the untreated VEGF188 tumour (Fig. 3).

4. Conclusions

Treatment with CA-4-P caused significant reduction in RBC velocity, with no recovery over 24 hours, in VEGF120 tumours, whereas VEGF188 tumours were much more resistant. However, pre-treatment with the tyrosine kinase VEGF receptor inhibitor, SU5416, modified the vasculature of VEGF120 tumours, such that RBC velocity was increased and response to CA-4-P was reduced. SU5416 had no effect on RBC velocity of VEGF188 tumours but also reduced their response to CA-4-P.

These data support the notion that presence of VEGF188 in tumours confers a level of protection from the effects of CA4P. It is thought that these tumours have a more mature stable vasculature which contributes to this protection (Tozer et al., 2008). The immature blood vessels in VEGF120 tumours are rapidly broken down. Tyrosine kinase inhibition with SU5416 significantly increased RBC velocity in individual vessels of VEGF120 tumours, which was accompanied by decreased vascularization (data not shown). SU5416 and similar agents were designed to block tumour angiogenesis by interfering with VEGF-mediated effects such as endothelial proliferation and migration. However, the current results support existing evidence that a sub-optimal anti-angiogenic effect can result in a rarefied tumour vascular bed, which nevertheless is efficiently perfused and capable of sustaining tumour growth (vascular normalization) (Jain, 2005). In addition, we show that vascular normalization can reduce the efficacy of the so-called vascular disrupting agents (VDAs), which are designed to target the established tumour vasculature. Further studies are required to investigate the vascular morphological changes that take place as a result of tyrosine kinase inhibition. It is possible that there is an increase in pericyte

coverage of these vessels, which would imply improved support and resistance against CA-4-P treatment. VEGF188 tumour response to CA-4-P was also reduced following SU5416 alone treatment, despite no effect of SU5416 on RBC velocity, and this result requires further mechanistic investigation, including analysis of vascular morphology.

This study shows that vascular normalization following anti-angiogenic treatment with a VEGF-R tyrosine kinase inhibitor can have unexpected consequences for subsequent treatment outcome. Analysis of RBC velocities in tumours, using the novel algorithm described, is a useful tool in measuring functional responses to vascular-targeted treatments.

Acknowledgements

Cancer Research UK funded this work.

5. References

Arteaga, C. L. (2003) Inhibiting tyrosine kinases: successes and limitations. *Cancer Biol Ther,* **2,** S79-83.

Baselga, J. (2006) Targeting tyrosine kinases in cancer: the second wave. *Science,* **312,** 1175-1178.

Blume-Jensen, P. & Hunter, T. (2001) Oncogenic kinase signalling. *Nature,* **411,** 355-365.

Drevs, J., Siegert, P., Medinger, M., Mross, K., Strecker, R., Zirrgiebel, U., Harder, J., Blum, H., Robertson, J., Jurgensmeier, J. M., Puchalski, T. A., Young, H., Saunders, O. & Unger, C. (2007) Phase I clinical study of AZD2171, an oral vascular endothelial growth factor signaling inhibitor, in patients with advanced solid tumors. *J Clin Oncol,* **25,** 3045-3054.

Ellis, L. M. & Hicklin, D. J. (2008) VEGF-targeted therapy: mechanisms of anti-tumour activity. *Nature Reviews Cancer,* **8,** 579-591.

Faivre, S., Demetri, G., Sargent, W. & Raymond, E. (2007) Molecular basis for sunitinib efficacy and future clinical development. *Nat Rev Drug Discov,* **6,** 734-745.

Folkman, J. (1990) What is the evidence that tumors are angiogenesis dependent? *J Natl Cancer Inst,* **82,** 4-6.

Fong, T. a. T., Shawver, L. K., Sun, L., Tang, C., App, H., Powell, T. J., Kim, Y. H., Schreck, R., Wang, X. Y., Risau, W., Ullrich, A., Hirth, K. P. & McMahon, G. (1999) SU5416 is a potent and selective inhibitor of the vascular endothelial growth factor receptor (Flk-1/KDR) that inhibits tyrosine kinase catalysis, tumor vascularization, and growth of multiple tumor types. *Cancer Res.,* **59,** 99-106.

Greco, O., Ireson, C., Coralli, C., Dachs, G., Shima, D. T., Steele, A., Tozer, G. M. & Kanthou, C. (2005) Role of VEGF and angiopoietins on tumour response to vascular disrupting agents. In: *NCRI Cancer Conference.* Birmingham.

Jain, R. K. (2003) Molecular regulation of vessel maturation. *Nat Med,* **9,** 685-693.

Jain, R. K. (2005) Normalization of tumor vasculature: an emerging concept in antiangiogenic therapy. *Science,* **307,** 58-62.

Parada, L. F., Land, H., Weinberg, R. A., Wolf, D. & Rotter, V. (1984) Cooperation between gene encoding p53 tumour antigen and ras in cellular transformation. *Nature,* **312,** 649-651.

Prazma, J., Carrasco, V. N., Garrett, C. G. & Pillsbury, H. C. (1989) Measurement of cochlear blood flow: intravital fluorescence microscopy. *Hear Res,* **42,** 229-236.

Reyes-Aldasoro, C. C., Akerman, S. & Tozer, G. M. (2008) Measuring the velocity of fluorescently labelled red blood cells with a keyhole tracking algorithm. *J Microsc,* **229,** 162-173.

Sandison, J. C. (1924) A new method for the microscopic study of living growing

tissues by the introduction of a transparent chamber in the rabbit's ear. *Anat. Rec.,* **28,** 281-287.

Shima, D. T., Kuroki, M., Deutsch, U., Ng, Y. S., Adamis, A. P. & D'Amore, P. A. (1996) The mouse gene for vascular endothelial growth factor. Genomic structure, definition of the transcriptional unit, and characterization of transcriptional and post-transcriptional regulatory sequences. *J Biol Chem,* **271,** 3877-3883.

Tischer, E., Mitchell, R., Hartman, T., Silva, M., Gospodarowicz, D., Fiddes, J. C. & Abraham, J. A. (1991) The human gene for vascular endothelial growth factor. Multiple protein forms are encoded through alternative exon splicing. *J Biol Chem,* **266,** 11947-11954.

Tozer, G. M., Akerman, S., Cross, N., Barber, P. R., Bjorndahl, M., Greco, O., Harris, S., Hill, S. A., Honess, D. J., Ireson, C. R., Pettyjohn, K. L., Prise, V., Reyes-Aldasoro, C. C., Ruhrberg, C., Shima, D. T. & Kanthou, C. (2008) Blood Vessel Maturation and Response to Vascular-Disrupting Therapy in Single Vascular Endothelial Growth Factor-A Isoform–Producing Tumors. *Cancer Res,* **68,** 2301-2311.

Tozer, G. M., Ameer-Beg, S. M., Baker, J., Barber, P. R., Hill, S. A., Hodgkiss, R. J., Locke, R., Prise, V. E., Wilson, I. & Vojnovic, B. (2005a) Intravital imaging of tumour vascular networks using multi-photon fluorescence microscopy. *Adv Drug Deliv Rev,* **57,** 135-152.

Tozer, G. M., Kanthou, C. & Baguley, B. C. (2005b) Disrupting tumour blood vessels. *Nat Rev Cancer,* **5,** 423-435.

Tozer, G. M., Prise, V. E., Wilson, J., Cemazar, M., Shan, S., Dewhirst, M. W., Barber, P. R., Vojnovic, B. & Chaplin, D. J. (2001) Mechanisms associated with tumor vascular shut-down induced by combretastatin A-4 phosphate: intravital microscopy and measurement of vascular permeability. *Cancer Res,* **61,** 6413-6422.

Unthank, J., Lash, J., Nixon, J., Sidner, R. & Bohlen, H. (1993) Evaluation of carbocyanine-labeled erythrocytes for microvascular measurements. *Microvascular Res,* **45,** 193-210.

Vieira, J. M., Schwarz, Q. & Ruhrberg, C. (2007) Selective requirements for NRP1 ligands during neurovascular patterning. *Development,* **134,** 1833-1843.

Winkler, F., Kozin, S. V., Tong, R. T., Chae, S. S., Booth, M. F., Garkavtsev, I., Xu, L., Hicklin, D. J., Fukumura, D., di Tomaso, E., Munn, L. L. & Jain, R. K. (2004) Kinetics of vascular normalization by VEGFR2 blockade governs brain tumor response to radiation: role of oxygenation, angiopoietin-1, and matrix metalloproteinases. *Cancer Cell,* **6,** 553-563.